Supplementary Materials

Repurposing of the anti-HIV drug Emtricitabine as a hydrogen-bonded cleft for bipyridines via cocrystallization

Gonzalo Campillo-Alvarado, Elizabeth A. Keene, Dale C. Swenson and Leonard R. MacGillivray*

Department of Chemistry, University of Iowa, Iowa City, IA, 52242-1294, USA.
e-mail: len-macgillivray@uiowa.edu

Supplementary Information:

S1. Materials and Instrumentation

S1.1. Materials

Emtricitabine (**FTC**) was purchased from Combi-Blocks Inc., 1,2-Bis(4-pyridyl)ethane (**bpeta**), 1,2-bis(4-pyridyl)ethylene (**bpe**), 4-azopyridine (**apy**) and 4,4′-bipyridine (**bipy**) and solvents were purchased from Sigma Aldrich. All reagents and solvents were used without further purification.

Cocrystals (**FTC**)$_2$·(**bpeta**), (**FTC**)$_2$·(**bpe**) and (**FTC**)$_2$·(**apy**) were obtained by combining **FTC** (40 mg, 0.162 mmol) with the corresponding bipyridine (0.081 mmol) through liquid-assisted grinding (LAG, methanol)[1] for 15 min. The resulting solids were dissolved in warm methanol (2 mL). Slow evaporation of the solution (2-3 days) afforded single crystals suitable for X-ray diffraction.

Cocrystal (**FTC**)$_2$·(**bipy**)$_2$·**H$_2$O** were obtained by combining **FTC** (40 mg, 0.162 mmol) with 4,4'-bipyridyl (25.3 mg, 0.162 mmol) through liquid-assisted grinding (LAG, methanol)[1] for 15 min. The resulting solids were dissolved in warm methanol (2 mL). Slow evaporation of the solution (2-3 days) afforded single crystals suitable for X-ray diffraction.

Instrumentation

Single crystal X-ray diffraction data were collected on a Bruker D-8 Venture diffractometer equipped with a Duo-Photon 3 area detector using Mo-Kα radiation ($\lambda_{MoK\alpha}$ = 0.71073 Å, diffraction source: Incoatec micro-source 3.0 Mo). The frames were integrated with the Bruker SAINT software package using a narrow-frame algorithm. Data were corrected for absorption effects using the Multi-Scan method (SADABS). Structure solution, refinement and data output were carried out with Olex2 software package[2] using XT, VERSION 2014/5 (solution using direct methods)[3] and XL, VERSION 2018/3 (refinement using full-matrix least-squares on F^2).[4] Non-hydrogen atoms were refined anisotropically and hydrogen atoms were placed in geometrically calculated positions using a riding model. Crystal structures were generated using Mercury.

Powder X-ray diffraction data were collected from samples mounted on a glass slide by a Bruker D8 Avance X-ray diffractometer using CuKα_1 radiation (λ = 1.5418 Å) typically in the range of 2θ = 5-35° (scan mode: continuous PSD fast; step size: 0.019°). The equipment was operated at 40 kV and 30 mA, and data were acquired at room temperature.

IR spectra have been recorded on a Thermo Scientific Nicolet 380 FT-IR spectrometer and measured in the range of 3600−750 cm^{-1} equipped with a diamond ATR crystal.

^{1}H NMR spectra were recorded using a Bruker AVANCE 300 NMR spectrometer operating at 300 MHz using DMSO-d_6 as solvent. Signal assignment for **FTC** was based on previous reports.[5] All data were processed with Mnova suite.

Methods

Force field intermolecular energy calculations were carried out using the UNI intermolecular potentials algorithm in CSD-Materials from the CCDC software package using the CIF files generated from single crystal X-ray diffraction refinement. Intermolecular energies within cocrystals were calculated for the highest-contributing intermolecular interactions.[6]

S2. Single-crystal X-ray diffraction data

Table S1. Crystallographic parameters for (**FTC**)$_2$·(**bpeta**), (**FTC**)$_2$·(**bpe**), (**FTC**)$_2$·(**apy**) and (**FTC**)$_2$·(**bipy**)$_2$·**H$_2$O**

Compound name	(**FTC**)$_2$·(**bpeta**)	(**FTC**)$_2$·(**bpe**)	(**FTC**)$_2$·(**apy**)	(**FTC**)$_2$·(**bipy**)$_2$·**H$_2$O**
Empirical formula	$(C_8H_{10}FN_3O_3S)_2$ ·$(C_{12}H_{12}N_2)$	$(C_8H_{10}FN_3O_3S)_2$ ·$(C_{12}H_{10}N_2)$	$(C_8H_{10}FN_3O_3S)_2$ ·$(C_{12}H_8N_4)$	$(C_8H_{10}FN_3O_3S)_2$ ·$(C_{10}H_8N_2)_2$·H_2O
Formula weight	678.73	676.72	677.69	824.895
Temperature/K	296.15	298.15	296.15	150.15
Crystal system	monoclinic	monoclinic	monoclinic	monoclinic
Space group	$P2_1$	$P2_1$	$P2_1$	$P2_1$
a/Å	7.6333(8)	7.4883(7)	7.5024(8)	7.4668(10)
b/Å	11.2359(11)	11.2957(11)	11.2194(11)	9.6700(14)
c/Å	18.1058(18)	18.1735(18)	18.2134(18)	26.187(4)
α/°	90	90	90	90
β/°	99.640(5)	100.406(5)	100.538(5)	90.087(4)
γ/°	90	90	90	90
Volume/Å^3	1531.0(3)	1511.9(3)	1507.2(3)	1890.8(5)
Z	2	2	2	2
ρ_{calc}g/cm^3	1.472	1.486	1.493	1.449
μ/mm^{-1}	0.243	0.246	0.249	0.215
F(000)	708.0	704.0	702.0	860.9
Crystal size/mm^3	0.185 × 0.055 × 0.05	0.145 × 0.065 × 0.03	0.13 × 0.095 × 0.02	0.115 × 0.1 × 0.06
Radiation	MoKα (λ = 0.71073)	MoKα (λ = 0.71073)	MoKα (λ = 0.71073)	Mo Kα (λ = 0.71073)
2Θ range for data collection/°	5.512 to 49.994	5.532 to 56.542	4.55 to 55.786	4.5 to 52.98
Index ranges	-9 ≤ h ≤ 9, -13 ≤ k ≤ 13, -21 ≤ l ≤ 21	-9 ≤ h ≤ 9, -14 ≤ k ≤ 13, -24 ≤ l ≤ 17	-9 ≤ h ≤ 9, -14 ≤ k ≤ 14, -23 ≤ l ≤ 23	-9 ≤ h ≤ 9, -12 ≤ k ≤ 12, -32 ≤ l ≤ 32
Reflections collected	15295	12872	32670	48450
Independent reflections	5271 [R_{int} = 0.0313, R_{sigma} = 0.0339]	6094 [R_{int} = 0.0238, R_{sigma} = 0.0337]	7064 [R_{int} = 0.0428, R_{sigma} = 0.0350]	7767 [R_{int} = 0.0550, R_{sigma} = 0.0423]
Data/restraints/parameters	5271/1/446	6094/1/417	7064/6/424	7767/49/508
Goodness-of-fit on F^2	1.024	1.059	1.073	1.038
Final R indexes [I>=2σ (I)]	R_1 = 0.0292, wR_2 = 0.0677	R_1 = 0.0369, wR_2 = 0.0838	R_1 = 0.0487, wR_2 = 0.1106	R_1 = 0.0559, wR_2 = 0.1267
Final R indexes [all data]	R_1 = 0.0325, wR_2 = 0.0700	R_1 = 0.0427, wR_2 = 0.0869	R_1 = 0.0591, wR_2 = 0.1157	R_1 = 0.0633, wR_2 = 0.1307
Largest diff. peak/hole / e Å^{-3}	0.14/-0.15	0.26/-0.19	0.48/-0.22	0.42/-0.39
CCDC deposition number	1981473	1981474	1981475	1981476

Table S2. Hydrogen bond and π···π contact parameters for (**FTC**)$_2$·(**bpeta**), (**FTC**)$_2$·(**bpe**), (**FTC**)$_2$·(**apy**) and (**FTC**)$_2$·(**bipy**)$_2$·**H$_2$O**.

Cocrystal	D–H···A/ Centroid···Centroid	*d*(D–H) [Å]	*d*(H···A) [Å]	*d*(D···A) [Å]	∠(D–H···A) [deg]	Symmetry code
(**FTC**)$_2$·(**bpeta**)	O1–H1···N7	0.817	2.024	2.838	174.11	-
	O4–H4A···N8	0.803	2.050	2.850	174.38	-
	N3–H3A···N5	0.867	2.126	2.989	173.93	-
	N6–H6A···N2	0.912	2.022	2.922	169.03	-
	N3–H3B···F1	0.867	2.482	2.766	99.83	-
	N6–H6B···F2	0.805	2.420	2.733	104.33	-
	C12–H12···F2	0.980	2.540	3.347	139.59	-x+2, y-1/2, -z
	C8–H8···O3	0.930	2.491	3.213	134.64	-x+2, y-1/2, -z+1
	C12–H12···F2	0.980	2.540	3.347	139.59	-x+2, y-1/2, -z
	C11–H11B···O6	0.970	2.472	3.291	141.93	-x+2, y+1/2, -z
	C3–H3C···N7	0.970	2.663	3.349	127.97	x+1, y, z
	C3–H3D···O3	0.970	2.461	3.417	168.47	-x+2, y-1/2, -z+1
	C28–H28···O6	0.930	2.592	3.342	137.95	-x+1, y+1/2, -z
	N3–H3B···O4	0.867	2.271	3.042	148.09	-x+1, y-1/2, -z
	N6–H6B···S1	0.805	2.759	3.516	157.35	-x+2, y+1/2, -z+1
	Cg1···Cg2[a]	-	-	3.918	-	-
	Cg3···Cg4[a]	-	-	3.682	-	-
(**FTC**)$_2$·(**bpe**)	O1–H1···N7	0.820	2.054	2.863	169.27	-
	O4–H4A···N8	0.820	2.044	2.858	171.24	-
	N6–H6A···N2	0.860	2.047	2.900	170.95	-
	N3–H3A···N5	0.860	2.108	2.965	174.03	-
	C16–H16···S2	0.930	3.007	3.621	124.94	-
	N3–H3B···F1	0.867	2.454	2.766	102.16	-
	N6–H6B···F2	0.860	2.412	2.735	102.85	-
	N6–H6B···S1	0.860	2.728	3.535	156.74	-x+2, y+1/2, -z+1
	N3–H3B···O4	0.860	2.774	3.024	145.74	-x+1, y-1/2, -z
	C8–H8···O3	0.930	2.455	3.174	134.22	-x+1, y-1/2, -z
	C16–H16···O6	0.930	2.630	3.322	131.65	-x+2, y+1/2, -z
	C12–H12···F2	0.980	2.495	3.299	139.17	-x+2, y-1/2, -z
	C3–H3C···N7	0.970	2.664	3.313	124.61	x+1, y, z
	C3–H3D···O3	0.970	2.470	3.428	169.35	-x+2, y-1/2, -z+1
	C18–H18···S2	0.930	3.019	3.877	154.09	-x+1, y-1/2, -z
	C11–H11B···O6	0.970	2.479	3.276	139.25	-x+2, y+1/2, -z
	C11–H11B···N8	0.970	2.680	3.348	126.37	x+1, y, z
	Cg1···Cg2[b]	-	-	3.798	-	-

	Cg3···Cg4[b]	-	-	3.666	-	-
(**FTC**)$_2$·(**apy**)	O1–H1···N7	0.820	2.074	2.886	170.26	-
	O4–H4A···N8	0.820	2.079	2.894	172.32	-
	N3–H3A···N5	0.860	2.109	2.964	172.55	-
	C14–H14···S2	0.930	2.927	3.552	125.79	-
	N6–H6A···N2	0.860	2.055	2.908	171.06	-
	N3–H3B···F1	0.860	2.457	2.766	102.07	
	N6–H6B···F2	0.860	2.412	2.734	102.80	
	C8–H8···O3	0.930	2.492	3.214	134.55	-x, y-1/2, -z+1
	N3–H3B···O4	0.860	2.331	3.093	147.84	-x+1, y-1/2, -z+2
	C12–H12···F2	0.980	2.489	3.299	139.83	-x, y-1/2, -z+2
	C11–H11B···O6	0.970	2.451	3.251	139.51	-x, y+1/2, -z+2
	N6–H6B···S1	0.860	2.746	3.545	155.23	-x, y+1/2, -z+1
	C3–H3C···O1	0.970	2.556	3.289	132.44	x-1, y, z
	C3–H3D···O3	0.970	2.447	3.408	170.69	-x, y-1/2, -z+1
	C9–H9···S1	0.930	2.818	3.616	144.63	x+1, y, z+1
	C26–H26···S1	0.930	2.582	3.330	137.77	-x+1, y+1/2, -z+2
	C9–H9···S1	0.930	2.934	3.787	153.13	-x+1, y-1/2, -z+2
	Cg1···Cg2[c]	-	-	3.755	-	-
	Cg3···Cg4[c]	-	-	3.688	-	-
(**FTC**)$_2$·(**bipy**)$_2$·**H$_2$O**	O1–H1···N7	0.840	1.968	2.786	164	-
	O4–H4A···N9	0.840	2.106	2.836	145	-
	O7–H7A···N10	0.870	2.053	2.851	152	-
	O7–H7B···O1	0.870	2.023	2.855	160	-
	N3–H3B···F1	0.880	2.443	2.762	101.87	
	N6–H6B···F2	0.880	2.432	2.754	102.05	
	N3–H3B···O1	0.880	2.281	3.097	105	1+x, y, z
	N3–H3A···O6	0.880	2.344	3.210	168	x, y, z-1
	N3–H3A···N5	0.880	2.357	3.028	133	1+x, y, z
	C4–H4···F1	0.880	2.308	3.122	137	-1+x, y, z
	Cg1···Cg2[d]	-	-	3.779	-	-
	Cg3···Cg4[d]	-	-	3.724	-	-

[a]Cg1 = N1, N2, C5–C8; Cg2 = N7, C17–C21; Cg3 = N4, N5, C13–C16; Cg4 = N8, C24–C28. [b]Cg1 = N1, N2, C5–C8; Cg2 = N7, C17–C21; Cg3 = N4, N5, C13–C16; Cg4 = N8, C24–C28. [c]Cg1 = N1, N2, C5–C8; Cg2 = N7, C17–C21; Cg3 = N4, N5, C13–C16; Cg4 = N8, C24–C28. [d] Cg1 = N7, C17–C21; Cg2 = N10, C27–C31; Cg3 = N8, C22–C26; Cg4 = N9, C32–C35.

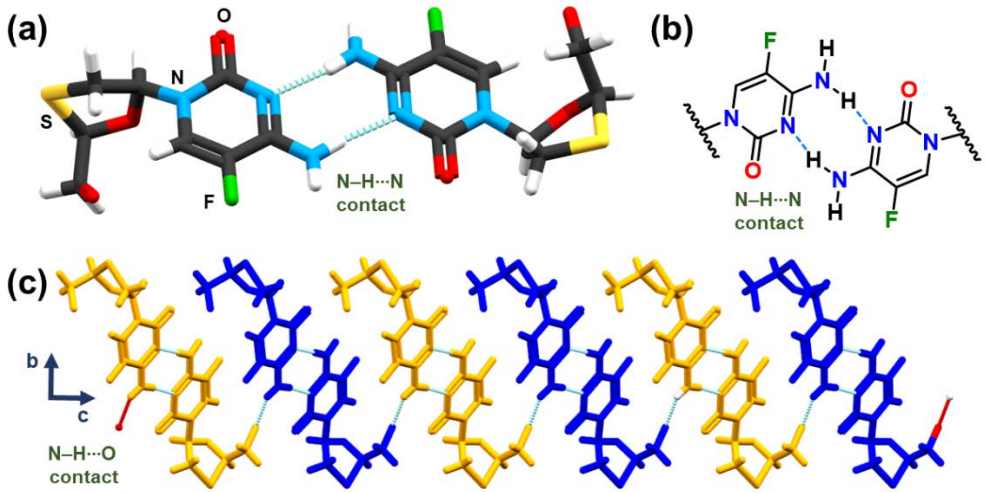

Figure S1. X-ray structure of FTC: (**a**) homodimer sustained by N-H⋯N hydrogen bonds, (**b**) two-point synthon, and (**c**) 1D ribbon sustained by N-H⋯O hydrogen bonds (CSD refcode: HAKJIM).[7]

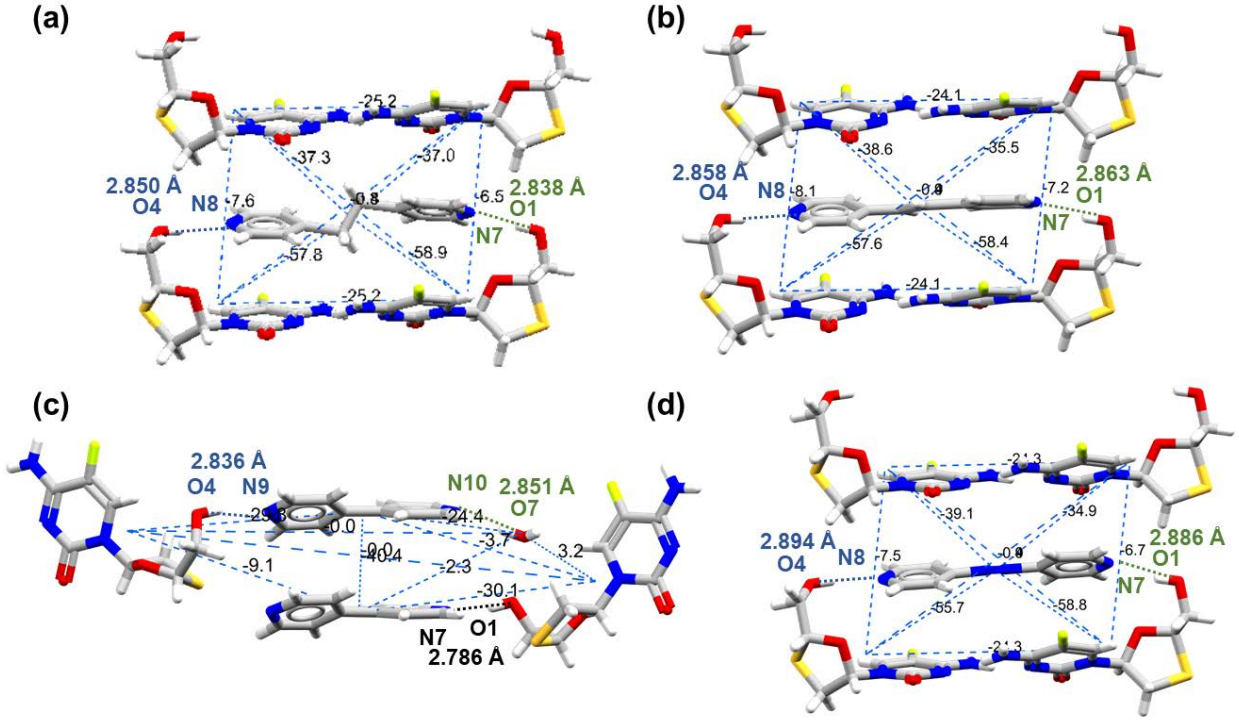

Figure S2. Intermolecular interaction energies (kJ mol^{-1}) and distances (Å) of highest-contributing interactions of crystal structures of (**FTC**)$_2$·(**bpeta**), (**FTC**)$_2$·(**bpe**), (**FTC**)$_2$·(**apy**) and (**FTC**)$_2$·(**bipy**)$_2$·**H$_2$O**.[6]

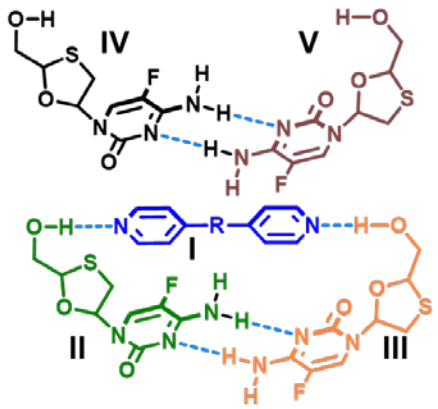

R = -(CH$_2$-CH$_2$), -(CH=CH), -(N=N)

Table S3. Selected intermolecular interaction energies (kJ mol^{-1}) for (**FTC**)$_2$·(**bpeta**), (**FTC**)$_2$·(**bpe**) and (**FTC**)$_2$·(**apy**).

Compound name / Intermolecular interaction energies of fragments (kJ mol^{-1})[1]	(**FTC**)$_2$·(**bpeta**)	(**FTC**)$_2$·(**bpe**)	(**FTC**)$_2$·(**apy**)	(**FTC**)$_2$·(**bipy**)$_2$·**H$_2$O**
I-II	-57.8	-57.6	-55.7	-
I-III	-58.9	-58.4	-58.8	-
I-IV	-37.3	-38.6	-39.1	-
I-V	-37.0	-35.5	-34.9	-
II-III	-25.2	-24.1	-21.3	-
Total packing energy	-443.0	-441.8	-432.0	-555.6

[1]Calculated based on the crystal structures containing highest occupancies in case of disorder.

S3. Powder X-ray diffraction (PXRD) data

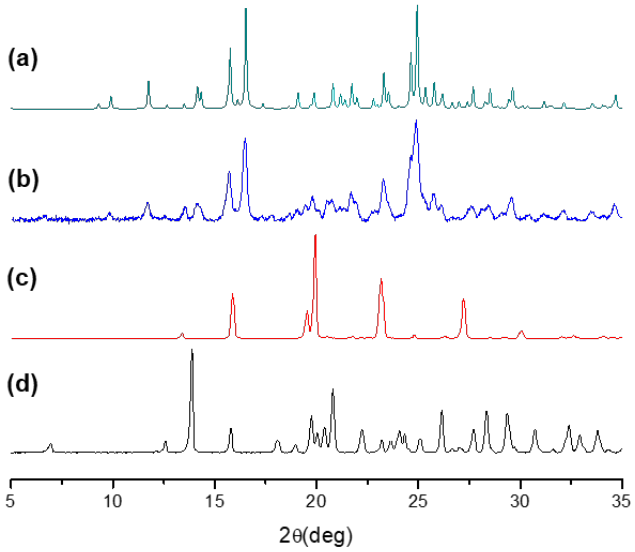

Fig. S3. PXRD analysis of (**FTC**)$_2$·(**bpeta**): (**a**) calculated powder pattern using single crystal X-ray data, (**b**) experimental powder pattern, (**c**) **bpeta** (experimental) and (**d**) **FTC** (experimental). Appearance of a new set of peaks in (**a**) and (**b**) compared to starting materials reflects the formation of a new solid phase.

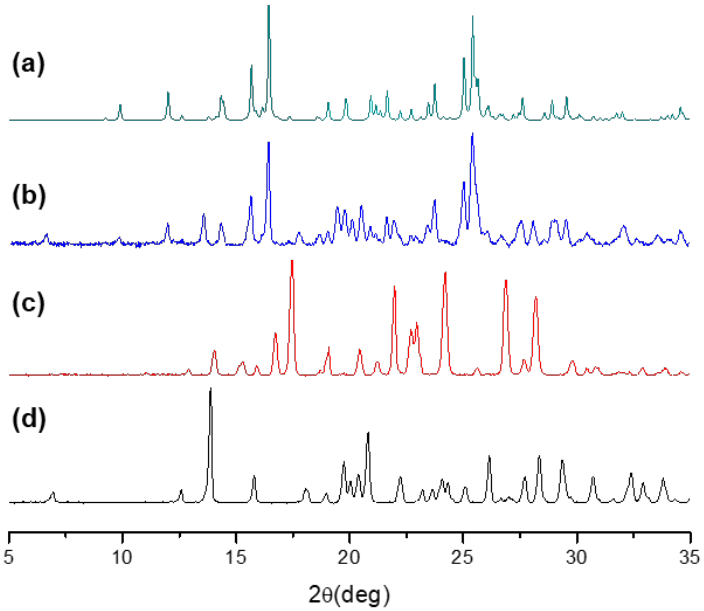

Fig. S4. PXRD analysis of (**FTC**)$_2$·(**bpe**): (**a**) calculated powder pattern using single crystal X-ray data, (**b**) experimental powder pattern, (**c**) **bpe** (experimental) and (**d**) **FTC**

(experimental). Appearance of a new set of peaks in (**a**) and (**b**) compared to starting materials reflects the formation of a new solid phase.

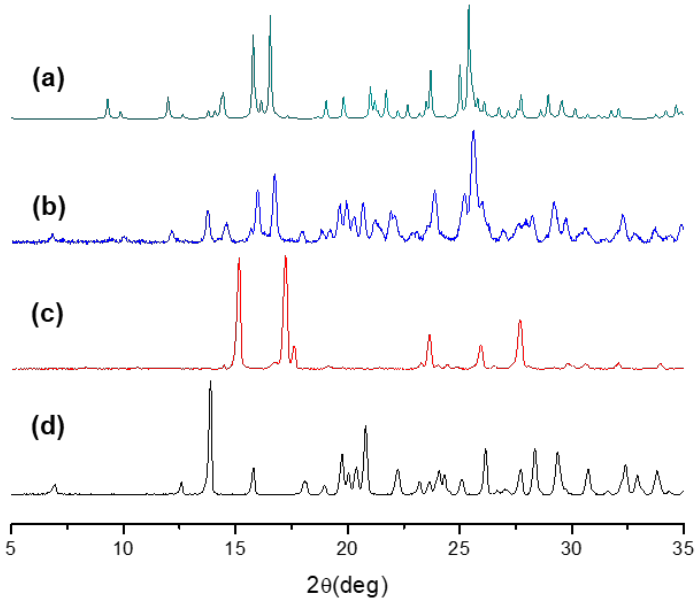

Fig. S5. PXRD analysis of (**FTC**)$_2$·(**apy**): (**a**) calculated powder pattern using single crystal X-ray data, (**b**) experimental powder pattern, (**c**) **apy** (experimental) and (**d**) **FTC** (experimental). Appearance of a new set of peaks in (**a**) and (**b**) compared to starting materials reflects the formation of a new solid phase.

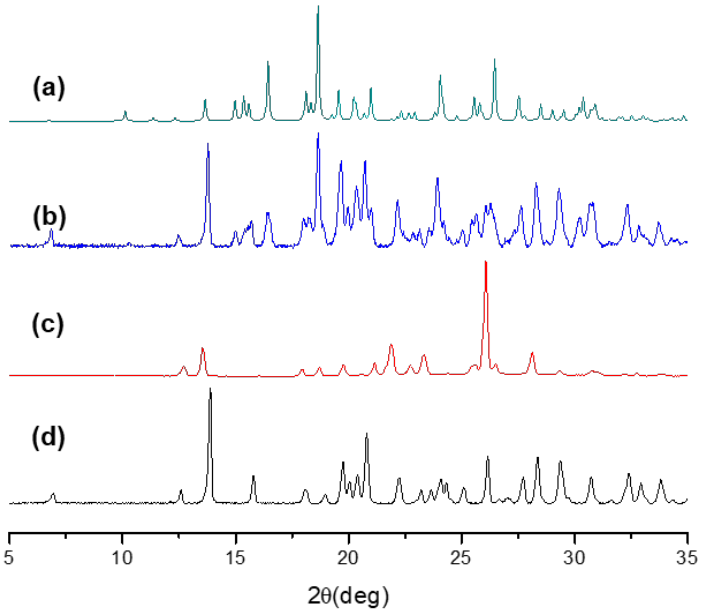

Fig. S6. PXRD analysis of (**FTC**)$_2$·(**bipy**)$_2$·**H$_2$O**: (**a**) calculated powder pattern using single crystal X-ray data, (**b**) experimental powder pattern, (**c**) **bipy** (experimental) and (**d**) **FTC**

(experimental). Appearance of a new set of peaks in (**a**) and (**b**) compared to starting materials reflects the formation of a new solid phase.

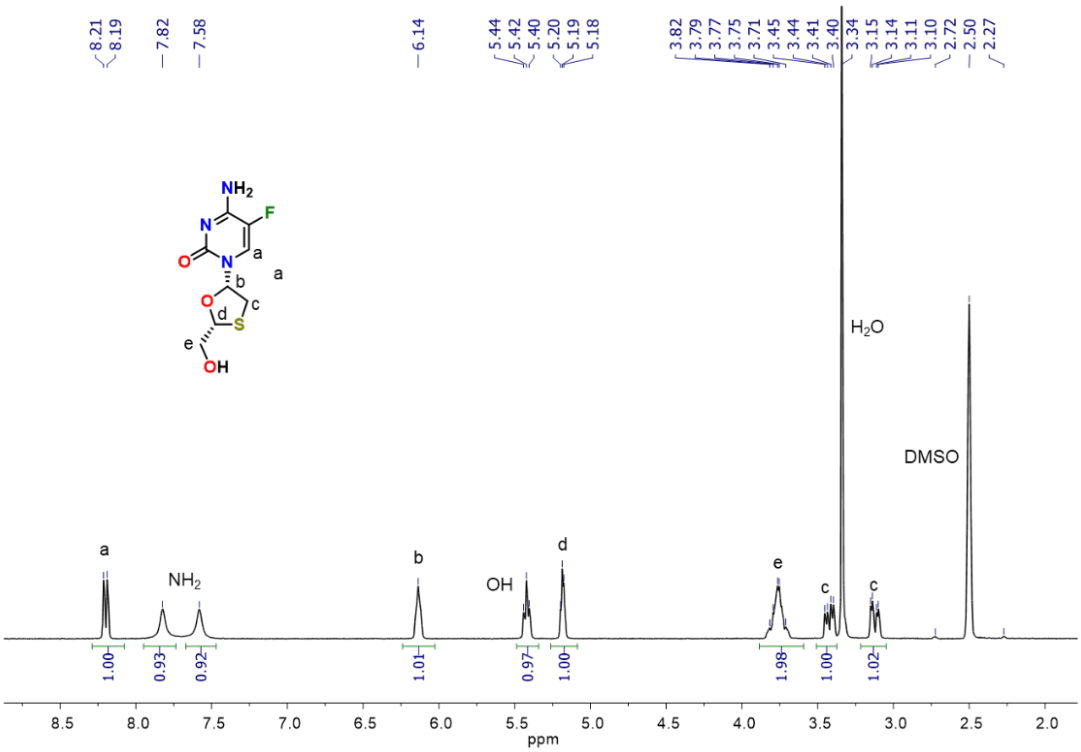

S4. ^{1}H NMR Data

Fig. S7. ^{1}H NMR spectra of **FTC** (300 MHz, DMSO-d_6, 16.18 mM, 26.85 ^{o}C).

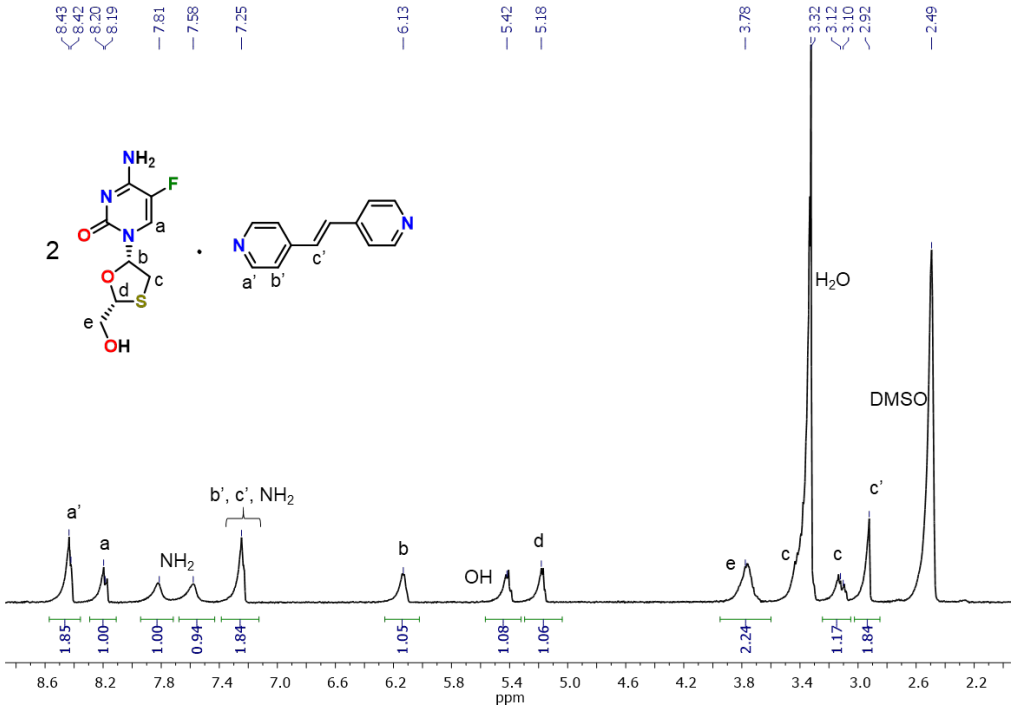

Fig. S8. ^{1}H NMR spectra of (**FTC**)$_2$·(**bpeta**) (300 MHz, DMSO-d_6, 9.28 mM, 26.85 ^{o}C).

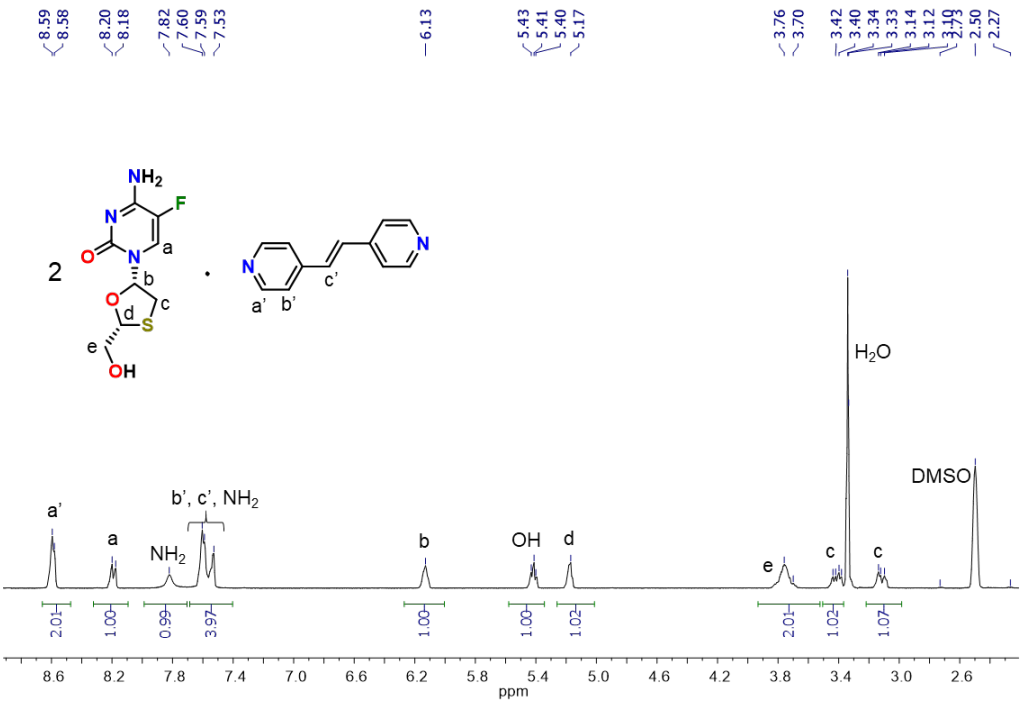

Fig. S9. ^{1}H NMR spectra of (**FTC**)$_2$·(**bpe**) (300 MHz, DMSO-d_6, 9.34 mM, 26.85 ^{o}C).

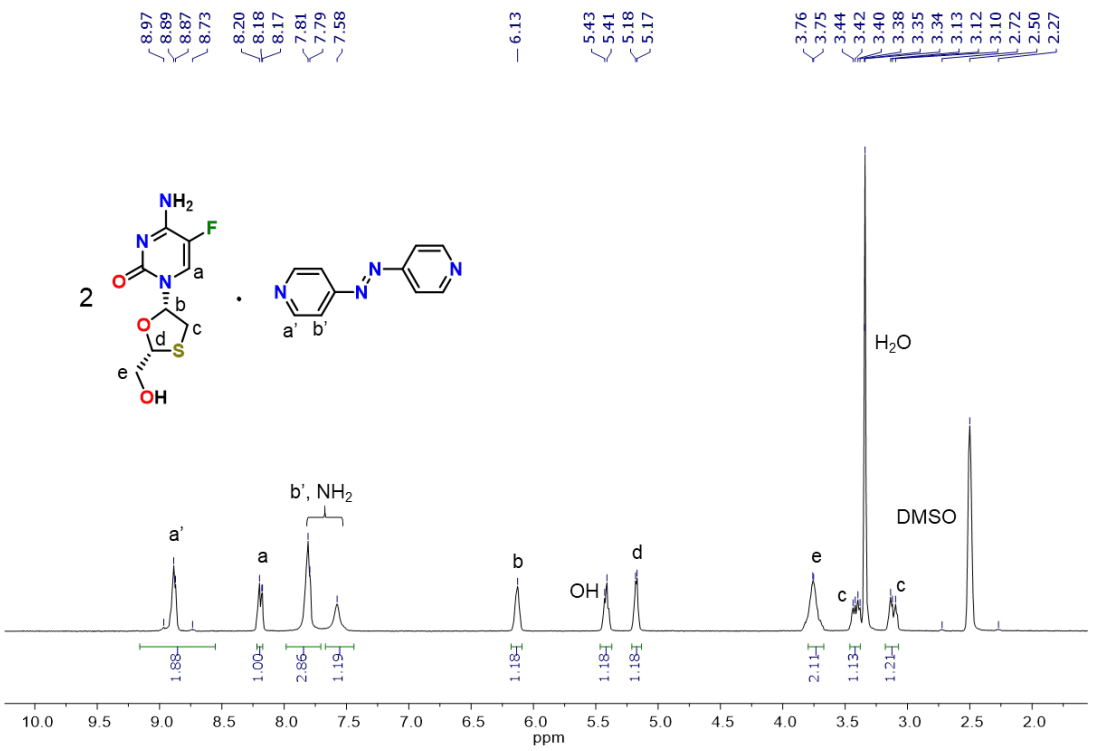

Fig. S10. ^{1}H NMR spectra of (**FTC**)$_2$·(**apy**) (300 MHz, DMSO-d_6, 9.28 mM, 26.85 ^{o}C).

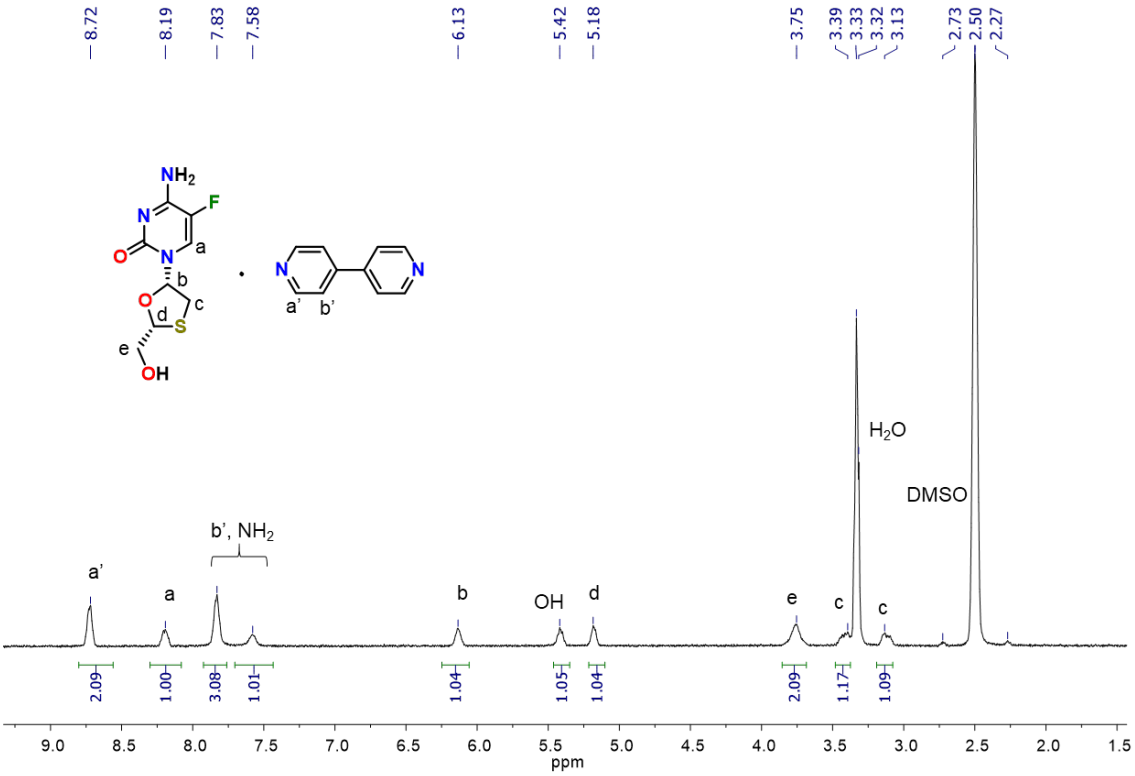

Fig. S11. ^{1}H NMR spectra of (**FTC**)$_2$·(**bipy**)$_2$·**H$_2$O** (300 MHz, DMSO-*d*$_6$, 14.16 mM, 26.85 ^{o}C).

S5. Attenuated Total Reflection Fourier Transform IR Spectroscopy Data

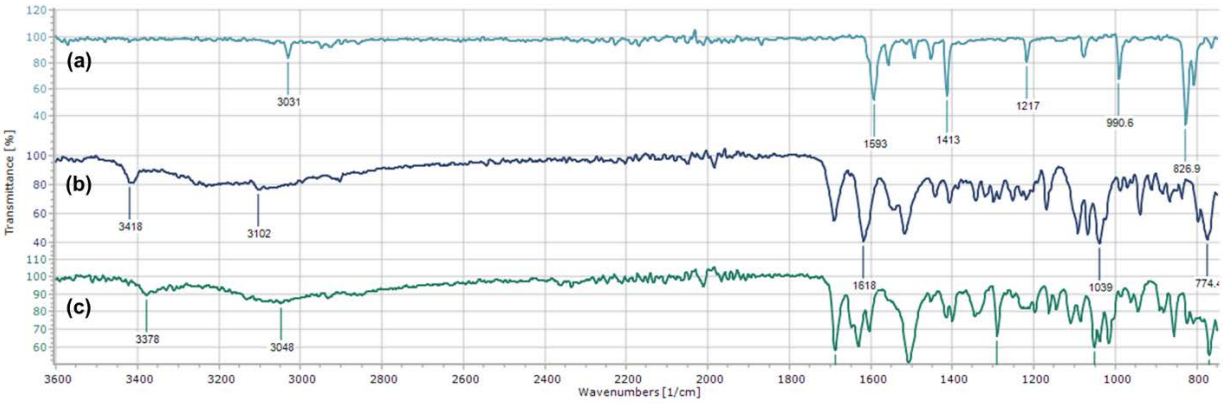

Fig. S12. ATR-IR spectrum of (**a**) **bpeta**, (**b**) **FTC** and (**FTC**)$_2$·(**bpeta**).

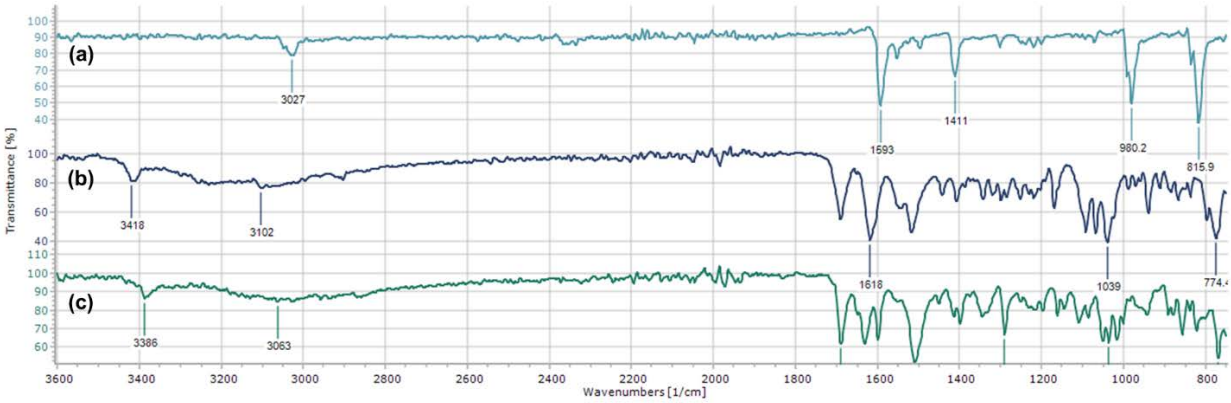

Fig. S13. ATR-IR spectrum of (**a**) **bpe**, (**b**) **FTC** and (**FTC**)$_2$·(**bpe**).

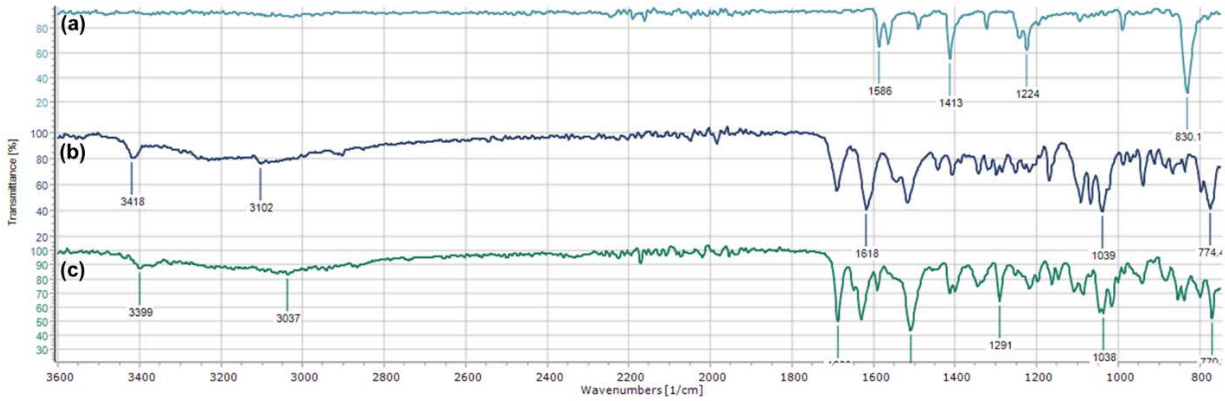

Fig. S14. ATR-IR spectrum of (**a**) **apy**, (**b**) **FTC** and (**FTC**)$_2$·(**apy**).

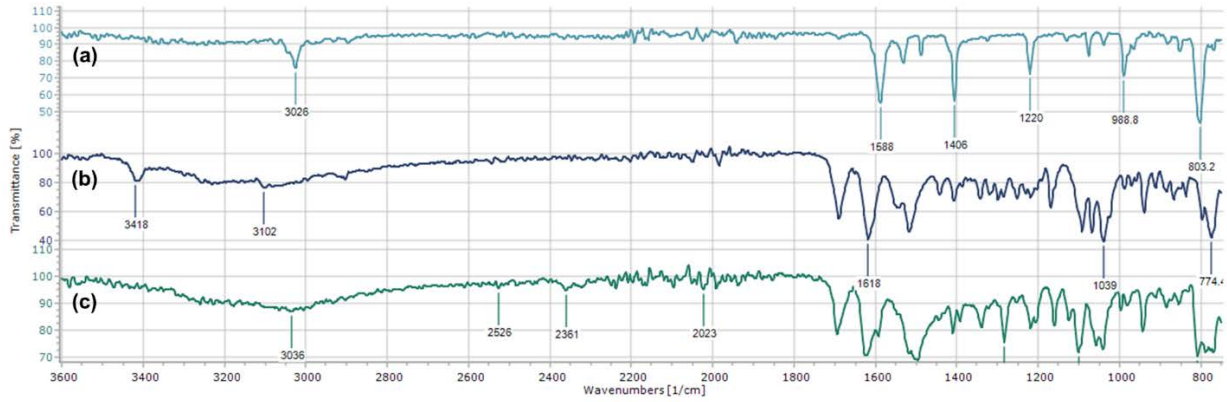

Fig. S15. ATR-IR spectrum of (**a**) **bipy**, (**b**) **FTC** and (**FTC**)$_2$·(**bipy**)$_2$·**H$_2$O**.

References

1. S. Karki, T. Friščić, W. Jones and W. D. S. Motherwell, *Mol. Pharm.*, 2007, **4**, 347-354.
2. O. V. Dolomanov, L. J. Bourhis, R. J. Gildea, J. A. Howard and H. Puschmann, *J. Appl. Crystallogr.*, 2009, **42**, 339-341.
3. G. M. Sheldrick, *Acta Cryst. A*, 2015, **71**, 3-8.
4. G. M. Sheldrick, *Acta Cryst. C*, 2015, **71**, 3-8.
5. (a) M. F. Caso, D. D'Alonzo, S. D'Errico, G. Palumbo and A. Guaragna, *Org. Lett.*, 2015, **17**, 2626-2629; (b) R. Nageswara Rao and K. Santhakumar, *New J. Chem.*, 2016, **40**, 8408-8417.
6. (a) A. Gavezzotti, *Acc. Chem. Res.*, 1994, **27**, 309-314; (b) A. Gavezzotti and G. Filippini, *J. Phys. Chem.*, 1994, **98**, 4831-4837.
7. P. van Roey, W. A. Pangborn, R. F. Schinazi, G. Painter and D. C. Liotta, *Antiviral Chem. Chemother.*, 1993, **4**, 369-375.